COBEM 2021 26th International Congress of Mechanical Engineering
November 22-26, 2021, Virtual Congress, Brazil
ABCM Associação Brasileira de Engenharia e Ciências Mecânicas

COB-2021-1702
CO-EXISTING ATTRACTORS IN HIGH FREQUENCY JARRING

Idin Nazzari
Saleh Amine Kehoul
Marcin Kapitaniak
Vahid Vaziri
Ekaterina Pavlovskaia
Marian Wiercigroch
Centre for Applied Dynamics Research, School of Engineering, University of Aberdeen, Aberdeen, AB24 3UE
i.nazzari@abdn.ac.uk

Abstract. *Low dimensional models of a typical multiple impact jarring tool are developed and studied to understand the effect of design and operational parameters on the tool's performance. These simple models comprised of lump masses, springs and viscous dampers, can mimic the tool main function of generating high amplitude impact forces from the energy stored in the pre-compressed spring. The magnitude and frequency of these impacts are controlled by the overpull and cam mechanisms respectively. The obtained numerical simulation results in form of bifurcation diagrams and basin of attractions, suggest that the system can exhibit co-exiting attractors, which can be explored to enhance the jarring tool performance by generating preferable impact force patterns.*

Keywords: *jarring, low-order modelling, parametric analysis, numerical analysis*

1. INTRODUCTION

A number of attempts have been undertaken to model jarring operations focused on prediction of the jar impact force and force at the stuck point (Skeem *et al.* 1979, Kalsi *et al.* 1987, and Moisyshyn and Levchuk 2016), optimisation of the jar placement, and estimation of loads conveyed to the drill-string as well as surface structures (Aarrestad and Kyllingstad 1994), where only a single impact cycle has been considered. However there have been indications that using high frequency impacts (Joppe *et al.* 2006) or vibration (Stoesz and DeGeare 2000), can in turn improve the performance of the jarring process despite applying lower overpull in the process. These publications do not report any examination of the possibility of multiple operating regimes that might develop due to non-linearity of impact itself, and therefore modelling of repeatable impacts in jarring becomes important. Impact oscillators and drifting oscillators appear to be promising in modelling high frequency impacts in jarring as they have been studied extensively in a wider context by Pavlovskaia *et al.* (2010), Liu *et al.* (2018) and Costa *et al.* (2020) among others to show co-existing solutions in similar systems and practicalities of controlling their dynamic responses. In this work a suitable impact oscillator model of jarring system is developed to predict optimum design, operational and environmental parameters. It is assumed that the tool performance could be enhanced by introducing high frequency impacts and maximising the transmitted force within the practical range of parameters in representative real life stuck tool scenarios.

2. MATHEMATICAL MODELLING

A typical jarring system, as shown in Figure 1(a), is modelled to mimic the dynamic behaviour of high frequency impacts. Interactions between the following three elements were considered: the stuck point, the jar tool (consisting of cams, hammer and anvil), and the topside drill-string where the overpull is applied. The jar tool excitation and impact cycles were assumed to have three phases: (i) *rest*, when the hammer and anvil are in contact and compressed, (ii) *lift*, when the hammer and anvil separate due to engagement of the cams, and (iii) *impact*, when the cams release, the hammer drops and hits the anvil. After the initial impact, the hammer might bounce and go through multiple impacts before it eventually rests compressed on the anvil due to the overpull. At this point the jar is back to the first stage and the cycle can repeat.

The overpull is applied on topside which is conveyed to the stuck point through the jar tool. Rotation of the drill string above the tool will cause the jar tool cams to engage, which in turn causes the hammer and anvil to separate. Upon drop of the cams, the hammer will hit the anvil and the tool resets prior to the subsequent lift cycle. The stuck point will experience the overpull, and the amplified force signal from the hammer and anvil impact.

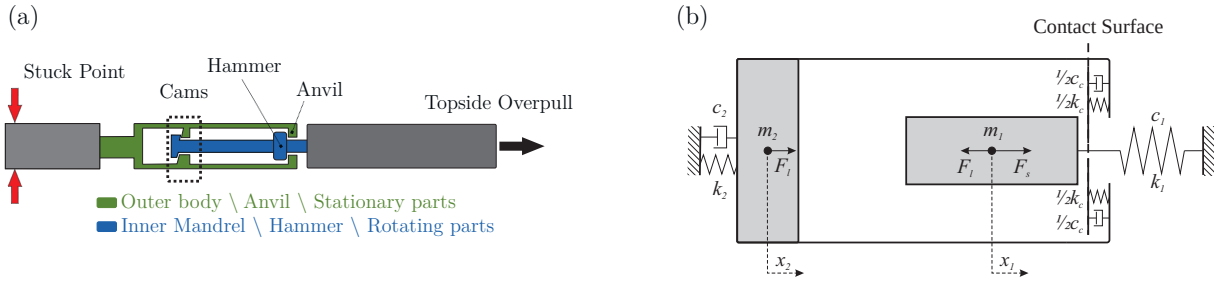

Figure 1. (a) A typical jar system with rotary excitation through cams arrangement, (b) 2-DOF physical model for hammer m_1 and anvil m_2 subject to static force F_s and dynamic force F_l

2.1 Two Degrees-of-Freedom Model

A two degrees-of-freedom low dimensional model is introduced to represent jarring dynamics and the hammer-anvil interaction (Figure 1(b)).

The hammer and anvil are represented by mass m_1 and m_2 respectively. The hammer is connected to a spring with a stiffness k_1 and damping coefficient c_1 simulating the topside drill-string behaviour. The anvil is connected to the stuck point, with a drill-pipe with stiffness k_2 and damping coefficient c_2. The jarring tool is generally closer to the stuck point than the topside, so it is expected for k_1 to be smaller than k_2 where both depend on the drill-pipe geometry and material. The coefficients c_1 and c_2 represent the structural damping of the drill-pipe with additional effect of energy dissipation due to friction, interaction with the drilling mud or hydraulic fluids within the tool. The hammer-anvil contact is modelled by assuming local deformation at the contact surface with linear stiffness k_c and damping coefficient c_c (Kelvin-Voigt model). Hammer and anvil displacements are described by x_1 and x_2.

The hammer is subject to a static force F_s replicating the topside overpull and the hammer-anvil separation is achieved by periodic lift force $F_l(t)$ acting on both the hammer and the anvil in opposite directions.

Through the 3 stages of the jar action, the hammer and the anvil will be in two arrangements that would change the equations of motion: when they are in contact and when they are not. The stages of jar action are replicated through the periodic changes of the lift force.

Case 1: Hammer and anvil not in contact

Hammer and anvil will not be in contact when $x_1 < x_2$. In this condition the equations of motion can be written as follows:

$$m_1\ddot{x_1} + c_1\dot{x_1} + k_1x_1 = F_s - F_l(t), \tag{1}$$

$$m_2\ddot{x_2} + c_2\dot{x_2} + k_2x_2 = F_l(t). \tag{2}$$

Equations can be non-dimensionalised with the following parameter changes:

$$z_1 = \frac{x_1}{l}, z_2 = \frac{x_2}{l}, \omega_c^2 = \frac{k_c}{m_1}, \tau = \omega_c t, \tag{3}$$

where l is maximum hammer lift (stroke length). It should be noted that in most hammer-anvil separation mechanisms such as a cams system or hydraulic pistons, the maximum stroke length is dictated by system geometry and thus can be used as a constant for non-dimensionalising. Note that the case condition $x_1 < x_2$ can be written as $z_1 - z_2 < 0$. Following parameters are defined to simplify the equations:

$$\kappa_1 = \frac{k_1}{k_c}, \kappa_2 = \frac{k_2}{k_c}, \eta = \frac{m_1}{m_2}, \quad \zeta_1 = \frac{c_1}{2m_1\omega_c}, \zeta_2 = \frac{c_2}{2m_1\omega_c}, \zeta_c = \frac{c_c}{2m_1\omega_c}, \quad f_s = \frac{F_s}{lk_c}, f_l(\tau) = \frac{F_l(t)}{lk_c}. \tag{4}$$

By substituting the parameters and simplifying the equations we obtain:

$$z_1'' + 2\zeta_1 z_1' + \kappa_1 z_1 = f_s - f_l(\tau), \tag{5}$$

$$z_2'' + 2\eta\zeta_2 z_2' + \eta\kappa_2 z_2 = \eta f_l(\tau). \tag{6}$$

where prime denotes derivatives in respect to non-dimensional time (τ).

Case 2: Hammer and anvil in contact

Hammer and anvil will be in contact when $x_1 \geq x_2$ or in non-dimensional terms $z_1 - z_2 \geq 0$. Using Kelvin-Voigt model the equation of motion can be written as follows:

$$m_1\ddot{x_1} + c_1\dot{x_1} + k_1x_1 = F_s - F_l(t) - (c_c(\dot{x_1} - \dot{x_2}) + k_c(x_1 - x_2)), \tag{7}$$

$$m_2\ddot{x_2} + c_2\dot{x_2} + k_2x_2 = F_l(t) + (c_c(\dot{x_1} - \dot{x_2}) + k_c(x_1 - x_2)) \tag{8}$$

Substituting the non-dimensional parameters introduced before, we obtain

$$z_1'' + 2\zeta_1 z_1' + \kappa_1 z_1 = f_s - f_l(\tau) - \big(2\zeta_c(z_1' - z_2') + (z_1 - z_2)\big), \tag{9}$$

$$z_2'' + 2\eta\zeta_2 z_2' + \eta\kappa_2 z_2 = \eta f_l(\tau) + \eta\big(2\zeta_c(z_1' - z_2') + (z_1 - z_2)\big). \tag{10}$$

2.2 One Degree-of-Freedom Model

It can be shown that for very large values of anvil mass m_2 ($\eta \to 0$) or large stiffness between the anvil and the stuck point k_2 ($\kappa_2 \to \infty$), the system can be reduced to a one degree-of-freedom model as the displacement of the anvil would be negligible (refer to Figure 2). With this assumptions the non-dimensional equation of motion can be re-written as:

$$z'' + 2\zeta z' + \kappa z = f_s - f_l(\tau) - H(z)(2\zeta_c z' + z), \tag{11}$$

where H is the Heaviside function:

$$H(x) = \begin{cases} 0, x < 0, \\ 1, x \geq 0, \end{cases} \tag{12}$$

and in absence of ζ_2 and κ_2, ζ_1 and κ_1 are changed to ζ and κ respectively.

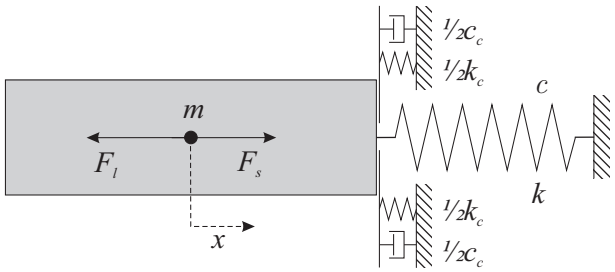

Figure 2. Physical 1-DOF model for hammer m_1 subject to static force F_s and dynamic force F_l.

2.3 Cam Lift Load

To avoid adding degrees-of-freedom to the system to represent position of the cams, it can be assumed that the connections between the cam-anvil and the cam-hammer interfaces are stiff enough so that the gap between of hammer and anvil represents the cams' position. The cams' interaction force can be seen as the force due contact interaction between two cams, with one surface moving on a linear path from zero to unit displacement for a fixed period of top rotation angle. Similar to hammer and anvil interaction, this contact can be formulated with Kelvin-Voigt model with linear stiffness and damping. To simplify the equations, we assume the cam-cam contact properties are the same as that of the hammer-anvil contact. Considering the shape of the cams, they can be assumed to be in contact between cam rotation angles ϕ_1 and ϕ_2. Using the assumptions made above we can write the lift force as

$$f_l(\tau) = H(r\tau - \phi_1)H(\phi_2 - r\tau)\big(z - (\alpha r\tau + \beta) + 2\zeta_c(z' - \alpha r)\big), \tag{13}$$

where r is the non-dimensional excitation frequency and α and β describe the expected linear lift position of the cams between ϕ_1 and ϕ_2. Since the lift position is zero at ϕ_1 and -1 at ϕ_2, α and β can be described as follows:

$$\alpha = \frac{-1}{\phi_2 - \phi_1}, \beta = \frac{\phi_1}{\phi_2 - \phi_1}. \tag{14}$$

However, this force needs to be set to zero when the actual displacement of the hammer (which translates to cam positions) is larger than the geometrically expected lifting of the cams. In this scenario the cams are no longer in contact and the force needs to be zero, so:

$$f_l(\tau) = H(r\tau - \phi_1)H(\phi_2 - r\tau)H\Big(z + \frac{r\tau}{\phi_2 - \phi_1} - \frac{\phi_1}{\phi_2 - \phi_1}\Big)\Big(z + \frac{r\tau}{\phi_2 - \phi_1} - \frac{\phi_1}{\phi_2 - \phi_1} + 2\zeta_c(z' + \frac{r}{\phi_2 - \phi_1})\Big). \tag{15}$$

3. BIFURCATION ANALYSIS

In this section we present the results of numerical studies carried out to determine the effect of the design, operations and environmental parameters on the tool performance in the one degree-of-freedom jar model. Our analysis shows that for given set of parameters more than one solution is available, where one might be more desirable to the operator in terms of the jarring performance. Careful selection of the tools design parameters or choice of operational parameters may allow the operator to drive the tool to reach the more desirable solutions.

Stuck pipes incidents by nature are not planned, so certain parameters are not in control of the operator. These may include the depth that the stuck pipe incident happens (drill-string length, affecting the drill-string stiffness), the type of drill-pipe soil interaction for example due to well angle (affecting the pipe damping ratio). However some aspects of the system affecting the damping ratio can be managed within a range of values, such as drilling mud density or viscosity.

The hydraulic and rheology properties also affect the cam/cam or hammer/anvil damping, but it is safe to assume that contact properties (stiffness and damping) are mainly functions of the shape and materials chosen, and thus can be seen as design parameters. The two main parameters that the operators have direct control over is the overpull and the frequency of excitation (angular velocity of top rotation in case of the cam mechanism described in the previous section).

In this work, we present parameters estimated based on assumption of the jar tool attached to the end of a 500 metre 6.5" steel drill pipe, with contact and damping assumptions taken such that resulted in the following values for the non-dimensional parameters: $f_s = 0.105$, $\kappa = 0.008$, $\zeta = 0.4$ and $\zeta_c = 0.25$. This set of parameters is used to demonstrate the range of system behaviours. Further parametric analysis is required to determine the envelope within which each of the system attractor types exist.

To understand the tool performance, two aspects will be focused on: maximum transmitted force to the stuck point (hammer-anvil interaction in 1DoF model) and the periodicity of the response with the consideration that periodic response could potentially help dislodge the stuck pipe by altering the stuck pipe-soil interaction for example by exciting the soil and rock particles causing the stuck pipe, where a chaotic response would be less effective in doing so. Both criteria can by proxy be studied by considering the maximum displacement of the hammer.

Figure 3 shows maximum amplitude of the system for range of non-dimensional frequencies from 0.1 to 1.5. It is expected that at low frequencies each hammer and anvil impact happens as an independent incident, as the hammer and anvil impact effect is dampened before next cam lift happens. However as shown in Figure 3, as the excitation frequency increases, there exists a solution where the cams might engage before the hammer hits the anvil. Comparison of the two solutions at $r = 0.50$ shows one of them to include hammer and anvil impact, and the second one where the hammer does not hit the anvil. Similarly at $r = 0.84$ a period-2 and period-4 solution co-exist where in one the impact is harder (or in other words the period-2 response has a higher maximum displacement which suggest higher transmitted force to the stuck point). Although in the latter case the jar operator may be able to distinguish the two solutions by the periodicity of the shock signals on topside, despite the difference in performance desirability the two period-one solutions at $r = 0.50$ frequency are not easily identifiable from their vibration signature. This necessitates further study of the development of the undesirable attractor to devise measures to avoid the non-impact solution by design, or by choice of operating parameters such as frequency and overpull.

Furthermore the pattern of period-1 solutions changes to chaotic solution between $r = 0.535$ and 0.6025 before a periodic-3 solution emerges. The chaotic solution reappears for different frequency windows. For example two periodic solutions co-exist at $r = 0.84$. By increasing the frequency and after a process that appears to be a cascade of period doubling, a chaotic response emerges as shown in the Poincaré map for $r = 0.86$. A similar pattern can be observed at frequencies in proximity of $r = 0.677$, 1.103 and 1.320. The chaotic response may be desirable if it results in higher transmitted force to the stuck point, but coupling the model studied here and the stuck pipe-soil interaction might suggest a periodic response is better suited to dislodge the stuck pipe.

Comparing the trajectory of solutions for frequencies $r = 0.50$, 0.84 and 1.10 shows that the hammer lift is significantly higher at $r = 1.10$ where it reaches up to 3 times the stroke length dictated by the cam. Although we have not included this in the low-order model, the physical constraint in the tool might not allow this extended travel length for the hammer or this may be detrimental to the structural integrity of the tool. Similar cautionary note can be made about the three solutions at $r = 0.76$ where the period-4 solution on the right hand panel provides higher maximum displacement and transmitted force every 4 periods, but it also shows lower minimum displacement compared to the other two solutions.

Study of the basins of attraction shown in Figure 4 confirms co-existence of the attractors at frequencies $r = 0.5, 076$ and 0.84, while on the other hand shows that a single chaotic or period-6 solutions exist at higher frequencies $r = 0.86$ and $r = 1.10$ respectively.

4. CONCLUSIONS

Low dimensional models of a typical multiple impact jarring tool are developed and studied to understand the effect of design and operational parameters on the tool's performance. These simple models comprised of lump masses, springs and viscous dampers, can mimic the tool main function of generating of high amplitude impact forces from the energy stored

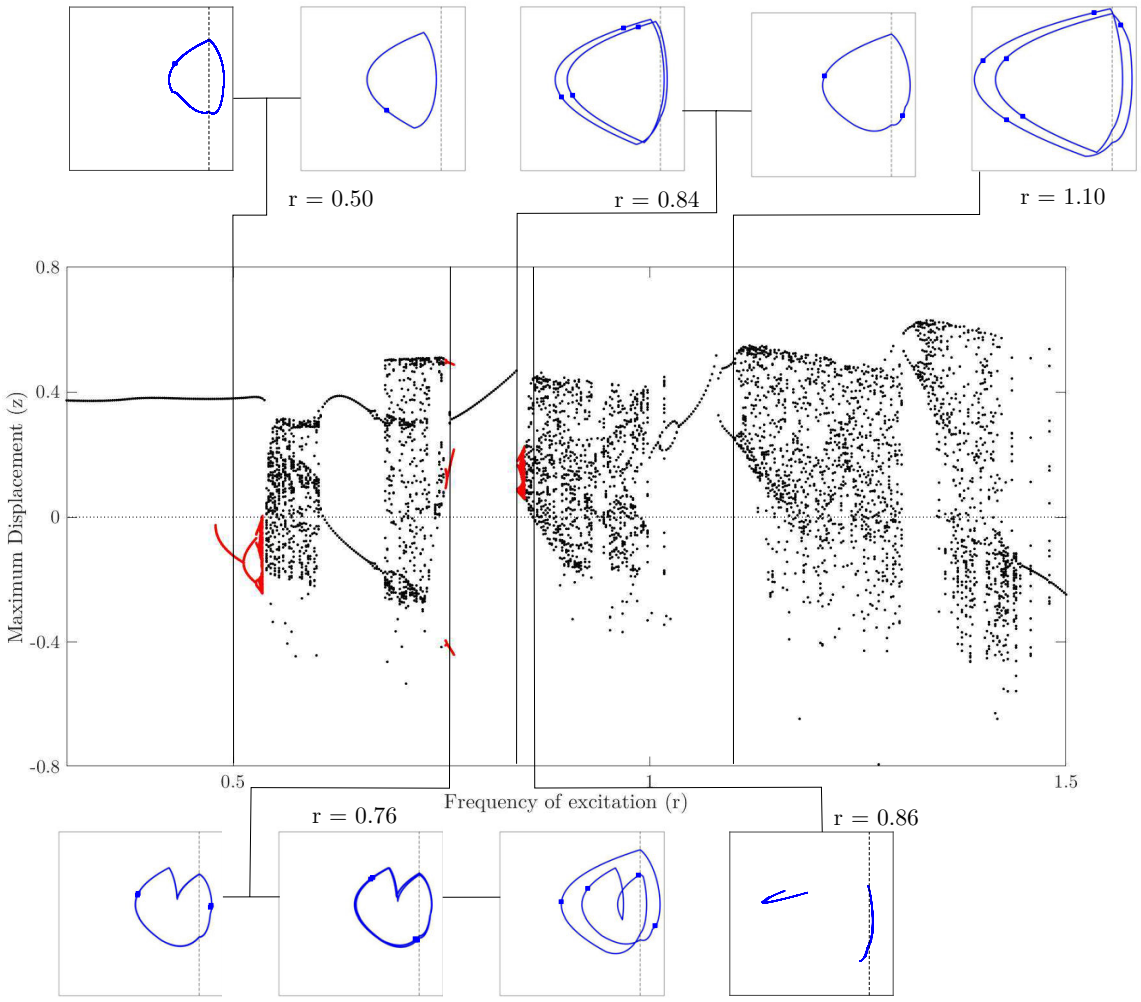

Figure 3. Bifurcation diagram showing maximum displacement of the jar hammer vs. excitation frequency for $f_s = 0.105$, $\kappa = 0.008$, $\zeta = 0.4$ and $\zeta_c = 0.25$. Co-existing attractors are shown with system trajectories on the phase plane (z, z') for frequencies $r = 0.50, 0.76, 0.84$ and 1.10. The Poincaré sections are marked on the trajectories with blue circles. The phase plane at $r = 0.86$ shows the Poincaré map. Hammer/anvil contact surface is shown in dashed lines at $z = 0$. Note that this bifurcation diagram only shows some of the solution branches. The forward sweep branches are shown in black colour and the red colour shows a sample of coexisting branches.

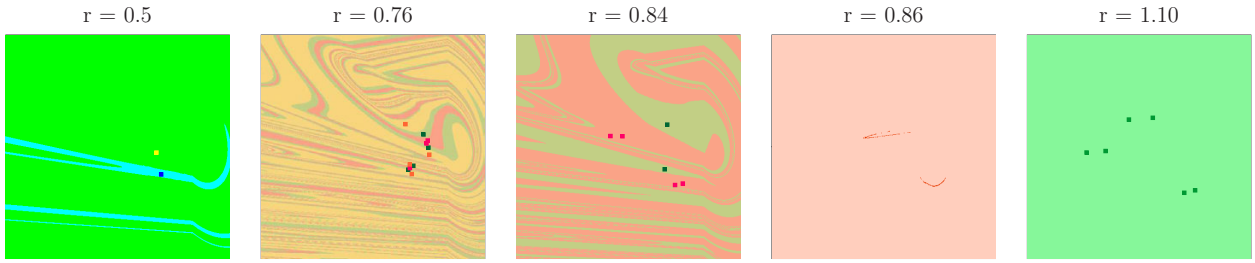

Figure 4. Basins of attraction for a sample of frequencies for $f_s = 0.105$, $\kappa = 0.008$, $\zeta = 0.4$ and $\zeta_c = 0.25$. The attractors are shown in Figure 3. Co-existing solutions are observed in frequencies $r = 0.5, 076$ and 0.84, and single chaotic and period six solutions are seen at $r = 0.86$ and $r = 1.10$ respectively.

in the pre-compressed spring. The models assume rigid body interaction between the hammer and anvil and between the cams. The model incorporates geometric constraints that allow the hammer to be lifted over a set distance (stroke length) and subsequently released each rotation cycle. The formulation of the hammer lift load is adjusted to take credit for cams' disconnection during the lift if the hammer/anvil or cam/cam interaction results in the hammer travelling faster than the velocity dictated by cams' rotation. The magnitude and frequency of hammer-anvil impacts are controlled by the overpull and cam rotation frequency respectively.

The numerical study of the model reveals co-existing attractors at certain frequencies. These co-existing solutions are not all desirable from the jarring operations perspective. For example we noticed that there exist solutions that have none or restricted hammer-anvil impact co-existing with solutions where the cams do not hinder the hammer drop on the cams. A careful study of the system parameters and sensitivity of the solutions to the environmental, design and operating parameters is required to determine a safe and effective operating envelope for the high-frequency jarring tool.

5. REFERENCES

Aarrestad, T.V. and Kyllingstad, Å., 1994. "Loads on drillpipe during jarring operations". *SPE Drilling & Completion*, Vol. 9, No. 04, pp. 271–275.

Costa, D., Vaziri, V., Kapitaniak, M., Kovacs, S., Pavlovskaia, E., Savi, M.A. and Wiercigroch, M., 2020. "Chaos in impact oscillators not in vain: Dynamics of new mass excited oscillator". *Nonlinear Dynamics*, Vol. 102, pp. 1–27.

Joppe, L.C., Mackenzie, G. and McGurk, M., 2006. "Using high-frequency downhole vibration technology to enhance through-tubing fishing and workover operations". In *SPE/ICoTA Well Intervention Conference and Exhibition*. SPE-99415-MS.

Kalsi, M., Wang, J. and Chandra, U., 1987. "Transient dynamic analysis of the drillstring under jarring operations by the fem". *SPE Drilling Engineering*, Vol. 2, No. 01, pp. 47–55.

Liu, Y., Paez Chavez, J., Pavlovskaia, E. and Wiercigroch, M., 2018. "Analysis and control of the dynamical response of a higher order drifting oscillator". *Proceedings of the Royal Society A: Mathematical, Physical and Engineering Sciences*, Vol. 474, No. 2210. 20170500.

Moisyshyn, V. and Levchuk, K., 2016. "The impact of vibration mechanism'installation place on the process of retrieving stuck drill pipe". *Mining of Mineral Deposits*, Vol. 10, pp. 65–76.

Pavlovskaia, E., Ing, J., Wiercigroch, M. and Banerjee, S., 2010. "Complex dynamics of bilinear oscillator close to grazing". *International Journal of Bifurcation and Chaos*, Vol. 20, No. 11, pp. 3801–3817.

Skeem, M.R., Friedman, M.B. and Walker, B.H., 1979. "Drillstring dynamics during jar operation". *Journal of Petroleum Technology*, Vol. 31, No. 11, pp. 1381–1386.

Stoesz, C.W. and DeGeare, J.P., 2000. "Low-frequency downhole vibration technology applied to fishing operations". In *SPE Annual Technical Conference and Exhibition*. SPE-63129-MS.

6. RESPONSIBILITY NOTICE

The authors are solely responsible for the printed material included in this paper.